



Anomalous transitions of DODAB using fast scanning liquid calorimetry

Lito P. de la Rama^a, Liang Hu^a, Mikhail Y. Efremov^b, Eric A. Olson^a, Paul F. Nealey^b, Mark A. McLean^c, Stephen G. Sligar^c, Leslie H. Allen^{a,*}

^a Department of Material Science and Engineering, University of Illinois - Urbana-Champaign, 1304 W Green St, Urbana, IL 61801, United States

^b Department of Chemical and Biological Engineering, University of Wisconsin - Madison, United States

^c Department of Biochemistry, University of Illinois - Urbana-Champaign, United States

ARTICLE INFO

Article history:

Available online 6 June 2011

Keywords:

Liquid calorimetry
DODAB phase transition
Protein calorimetry

ABSTRACT

Anomalous melting transitions are observed on dimethyl dioctadecyl ammonium bromide (DODAB) using a fast-scanning liquid calorimeter. A single transition is observed at low scan rates (1 K/min) while up to four peaks are evident at high scan rates (60 K/min). These deconvoluted transitions are signatures of the basic properties of the transition kinetic landscape which are convoluted into a single peak at low scanning rates. The technique is also applied to the proteins Rnase A, Lysozyme and Cytochrome P450. The calorimeter is a glass capillary uniformly coated with Ag, which acts both as the heating element and resistive thermometer.

© 2011 Elsevier B.V. All rights reserved.

1. Introduction

The core material physics of biological systems such as protein folding are often buried by the nature of the measurement method. Theoretical models have predicted multiple intermediate states in the unfolding process [1]. The path of the overall transition follows a kinetic landscape involving many steps – each step kinetically driven by their own time constant and activation energy. Computer simulations of Lysozyme unfolding show that the different secondary structures unfold at different times [2]. The unfolding of Cytochrome P450 has also been proposed to occur with at least three intermediate states [3].

However, measurements of these interesting but buried phenomena have yet to be realized. Therefore, it is useful to probe these materials using a fast scanning method which has access to a broad range of measurement time-scales. This may provide a gateway to deconvolute the basic steps of the transition process.

Thermal analysis has been a useful method in characterizing and uniquely labeling biological systems (i.e. determining the enthalpy, H_m , and temperature of the transition, T_m). However, current liquid calorimetry methods have limited utility in probing the multistep processes since the scanning rate of most conventional systems is too slow – 1 K/min. Recently, progress has been made in developing devices with low sample volume but little has been reported regarding expanding the range of scanning rates [4–10].

In recent years adiabatic MEMS-based fast scanning nanocalorimeters with picojoule sensitivity have been devel-

oped [11–13] and applied to various material systems including “magic” number studies in metal nanoparticles [14,15], polymer thin films [16], and self assembled alkanethiol lamella [17]. Recently, we have been able to measure the melting transition for a single layer alkanethiolate lamellar crystal synthesized on our nanocalorimetry sensor using gas phase methods [18]. However, the application of this method is limited to the thin film samples that are stable in vacuum. This method is not applicable to most biological systems of interest (denaturation of biological macromolecules like proteins and DNA, vesicle formation of lipids, and binding of small molecules to enzymes) since these materials are usually in the form of dilute aqueous (liquid) solutions. Conventional calorimeters which are now commercially available have heating rates of several hundred of K/min and can be used to study organic systems. However, these systems are not typically applied to liquid solutions. Specialized liquid calorimeters are commercially available but require relatively large amounts of samples and perform at slow heating rates. For example, the Microcal™ Cap-DSC system has a cell volume of 130 μ L and achieves a heating rate only up to 4 K/min.

In this paper, we present a capillary-based liquid calorimeter with fast heating rate. It features a calorimetric cell with $30 \pm 2 \mu$ L sample volume. High scanning rates are limited only by the radial temperature gradient in the capillary-enclosed sample. Only inert glass surface is in contact with the sample during the test. The working element of the tool – metalized glass capillary – can be made by a simple one-step metallization procedure.

We investigate the phase transitions of a model system dimethyl dioctadecyl ammonium bromide (DODAB) and proteins such as Rnase A, Lysozyme and Cytochrome P450. At low scan rates the thermal transitions of all of the material are consistent with those

* Corresponding author. Tel.: +1 217 333 7918.

E-mail address: l-allen9@illinois.edu (L.H. Allen).

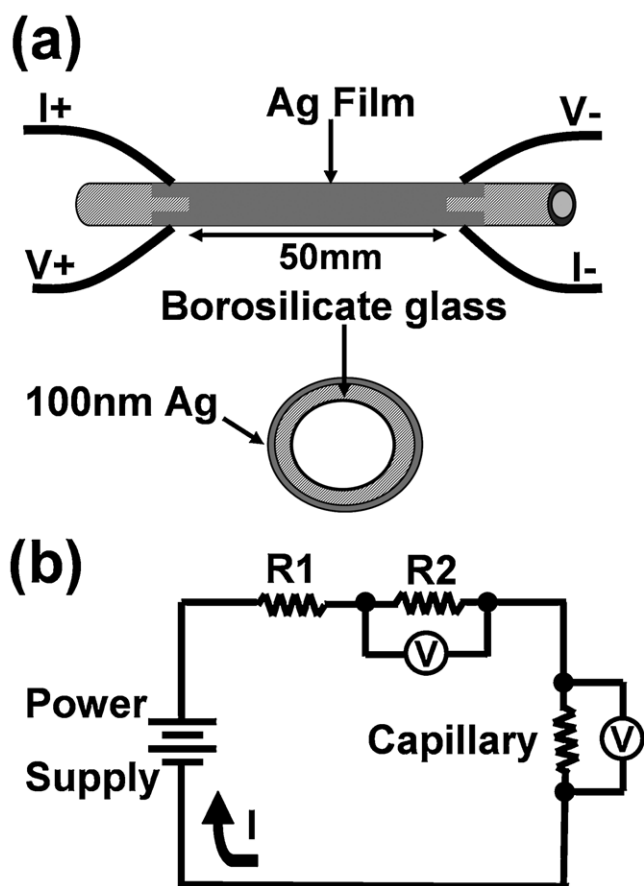


Fig. 1. (a) Schematic and cross-sectional profile of the capillary calorimeter cell. Small silver wires are used to connect the thin film heater to the 4-point probe resistance meter. (b) Circuit diagram of the calorimeter. R2 is composed of Vishay™ resistors with low temperature coefficient of resistivity (TCR).

obtained with slow scanning rates using conventional calorimeters. Values of T_m and H_m match those posted in the literature using conventional calorimeters such as Microcal™ system which is used in this study as the standard measurement technique.

2. Experimental

2.1. Liquid calorimeter device fabrication and operation

The liquid calorimeter device consists of a glass capillary uniformly coated with Ag as shown in Fig. 1. In detail, the calorimeter is made of borosilicate-glass capillary with an inner diameter of 0.90 mm, wall thickness of 0.25 mm and length of 10 mm as shown in Fig. 1(a). A 100 nm thin film of silver with 10 nm chromium adhesion layer is deposited on the surface of a 50 mm segment via thermal evaporation. A uniform thickness is achieved by rotating the capillary during evaporation. The Ag thin film serves both as a heater and as an RTD thermometer. Stable electric characteristics of the coatings are achieved by annealing them in vacuum of $\sim 10^{-7}$ Torr at 200 °C for 12 h followed by burn-in in the typical experimental conditions for several heating cycles. Custom-made liquid feedthrough to the vacuum chamber allows external injection of a liquid sample using a syringe pump. The open ends of the capillary are connected to the feedthrough via PTFE and polyolefin heat-shrink tubes.

The Ag coating is patterned with four pads that are in mechanical contact with 25 μm diameter silver wires for 4-point probe resistance measurements. The circuit diagram of the measurement

set-up is shown in Fig. 1(b). DC power supply (HP 3632 A) voltage is fixed to 30 V. The current limiting resistor R1 is the combination of low TCR metal foil resistors (Vishay Inc.) and determines the heating rate. The resistance of R1 is varied from 100 to 300 Ω which corresponds to the heating rate from 60 to 6 °C/min. The current through the cell I is calculated from the voltage drop across a 5 Ω resistor, R2. The voltage drop across the cell V is measured using a high precision digital voltmeter (HP 3458). The cell resistance, $R = V/I$ (typical values are around 5 Ω), is used to calculate the temperature of the cell via the temperature-resistance calibration curve obtained beforehand for each cell. A class A Pt RTD (Omega Inc.) is used as the temperature reference during the calibration.

The temperature uniformity of the device during operation is expected to be very excellent at the heating rates used in the experiment. The degree of temperature uniformity is limited by the radial temperature gradient in the capillary-enclosed sample which is controlled in part by the low thermal conductivity of water. The maximum temperature gradient is between the solution at the center of the capillary and the thin film heater. Thus, uniform temperature is achieved by the designing the capillary with a small diameter. In our case, the thermal time constant (τ_{th}) calculated using the diffusion equation for this system is negligibly small ($\tau_{th} \ll 1$ s) with the maximum temperature variation of only $\Delta T \sim 0.3$ K at 40 K/min heating rate.

Measurements of the sealed capillary are performed in vacuum of 10^{-3} to 10^{-7} . The calorimeter operates typically in the range of 20–80 °C with a temperature resolution of 0.1 °C. This resolution is maintained at the higher scan rates by increasing the reading rate from 36 readings/min for slow scans to 720 readings/min for fast scans. The heat capacity of the calorimetric cell is calculated as follows:

$$C_p = \frac{dU}{dt} = \frac{\text{power} \times \Delta \text{time}}{\Delta T} = \frac{I \times V \times \Delta \text{time}}{\Delta T} \quad (1)$$

The C_p of the sample is determined from the difference between the C_p of the solution and the C_p of the solvent. The C_p of the solvent is approximated as a fourth order polynomial fit to the plot of C_p as a function of temperature. Correction for heat loss is also accounted in this baseline subtraction.

2.2. Sample preparation

Four aqueous solutions of different biological materials are used in this study. DODAB is a model organic system which forms large polydispersed vesicles that mimic the membrane which constitute the walls of biological cells [19]. A solution in deionized water (18.2 M Ω cm resistivity at 25 °C) is heated up to 60 °C for 30 min with constant vigorous stirring following the reported preparation method for vesicle formation [20]. The Rnase A from bovine pancreas and Lysozyme from chicken egg white were purchased from Sigma and used without further purification. Solutions are prepared using 40 mM glycine/HCl buffer at pH 2.5 as solvent and filtered with a 0.22 μm syringe filter prior to use. Cytochrome P450 is a heme-cofactor containing enzyme which is involved in the synthesis and reactions of lipids and steroids and the first line of defense against drugs and xenobiotics [21]. It is dissolved in 0.1 mM phosphate buffer at pH 7.4 and dialyzed prior to use.

3. Results and discussion

Calorimetry results using scan rates of ~ 10 K/min for DODAB are shown in Fig. 2. The heat capacity (C_p) data for a 3 mM solution of DODAB averaged over 65 samples is shown in Fig. 2a. As expected the main phase transition is detected at $T_m = 45$ °C and attributed to the transition from an ordered gel phase to a liquid crystalline phase [22]. A smaller peak at 37 °C is attributed to a sub-

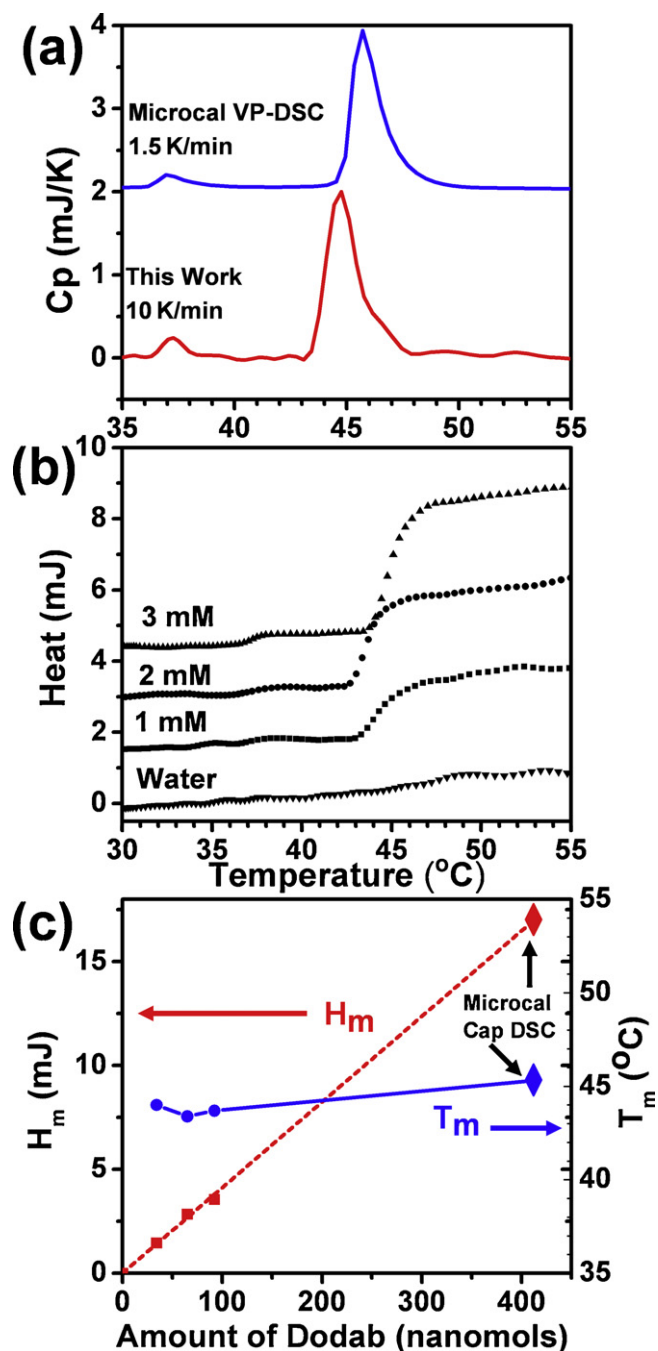


Fig. 2. (a) Heat capacity of an aqueous solution of DODAB with phase transition at 45 °C and a smaller pre-transition peak at 37 °C. (b) Plot of the heat applied to the system for 3 different DODAB concentrations (1 mM, 2 mM and 3 mM). The plot for the pure solvent (water) is plotted for comparison. Plots have been offset on the vertical scale for clarity. (c) Heat of transition of DODAB as a function of concentration showing a good linear trend. The transition temperature is also plotted showing consistent results on different samples. Data at 400 nmol is from a Microcal Cap-DSC calorimeter.

gel pre-transition [23]. These results are the same as those obtained using conventional liquid calorimeters operating at their maximum scan rate of 4 K/min. The measured values of the heat of transition $\Delta H_m = 42$ kJ/mol and T_m are consistent with the reported values ($T_m = 42$ –45 °C and $\Delta H_m = 40$ –50 kJ/mol) [19,22,23]. As shown in Fig. 2c, the value of H_m (mJ) scales directly with molar concentration of DODAB while T_m is independent of molar concentration over the range of concentration investigated.

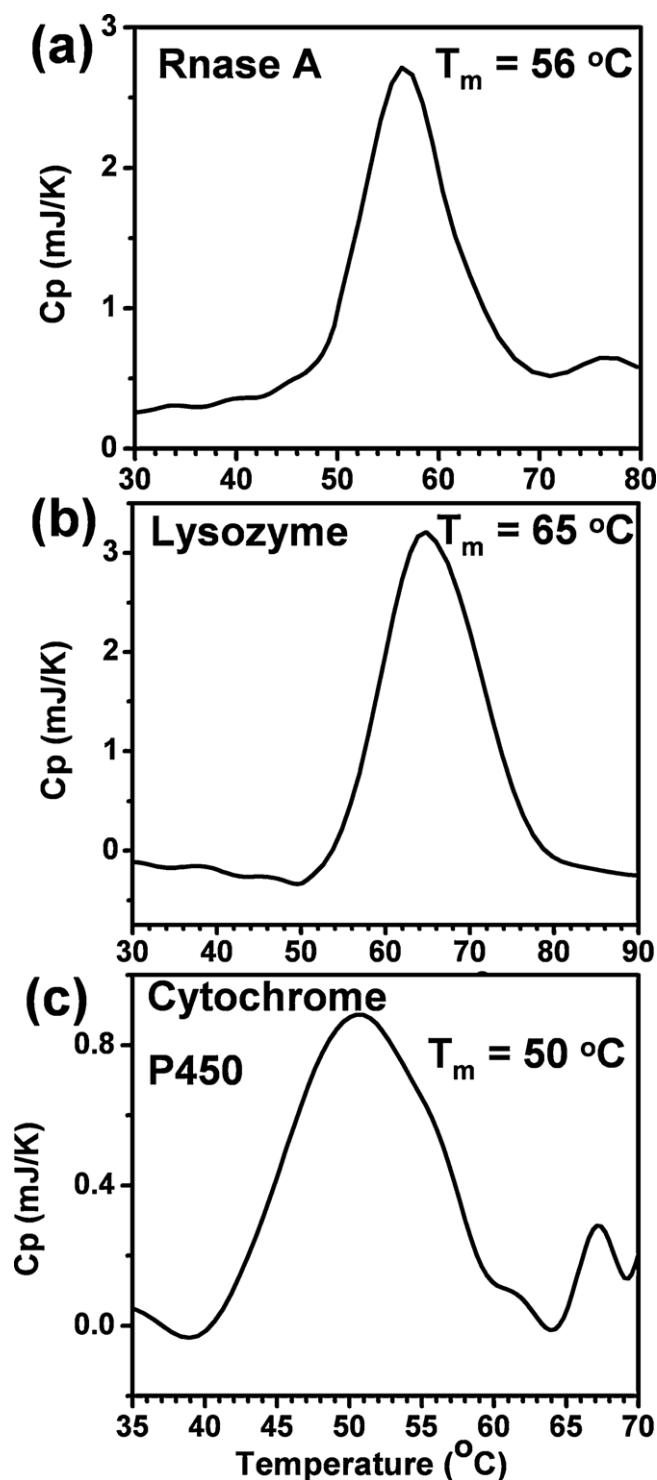


Fig. 3. (a) Heat capacity plot for Rnase A with a total sample size of 66 nmol in the capillary cell. (b) Plot for 89 nmol of Lysozyme. (c) C_p plot for 8 nmol of Cytochrome P450. Broad peak transitions are consistent with protein unfolding behavior.

Fig. 3 shows the heat capacity plots for the three protein test systems averaged over 10 samples. The plots show a very broad transition peak associated with the unfolding of the protein structure. Table 1 shows a good agreement between our device and the industry standard Microcal™ VP-DSC. These calorimetry data of DODAB and proteins indicate that at slow rates our 30 μ L calorimeter gives results which are the same as conventional systems even though the volume of solution is much lower.

Table 1
Results comparison with Microcal™ VP-DSC.

Test system	T_m (°C)		ΔH (kJ/mol)	
	This work	Microcal	This work	Microcal
Dodab	45	45	42	42
Rnase A	56	56	310	342
Lysozyme	65	66	525	510
Cytochrome P450	50	48	1000	970

A key new finding is that when the calorimetry analysis is done at high scan rates – multiple transitions are observed (DODAB). As shown in Fig. 4a, the nature of the transition for DODAB changes progressively from a single transition to multiple transitions (peaks) as the scan rate increases. We used the multiple-peak fitting model in the Origin™ data analysis software for peak deconvolution into 4 separate peaks as shown in Fig. 4b. The overall transition at 40 K/min separates into 4 different peaks with the onset and maxima for each separated by ~ 1 K. Note that the transition does not just broaden as would be expected from instrumentation effects (e.g. thermal lags) but the transition deconvolutes into distinctly separate processes at high rates. The total integrated transition enthalpy is approximately the same for both

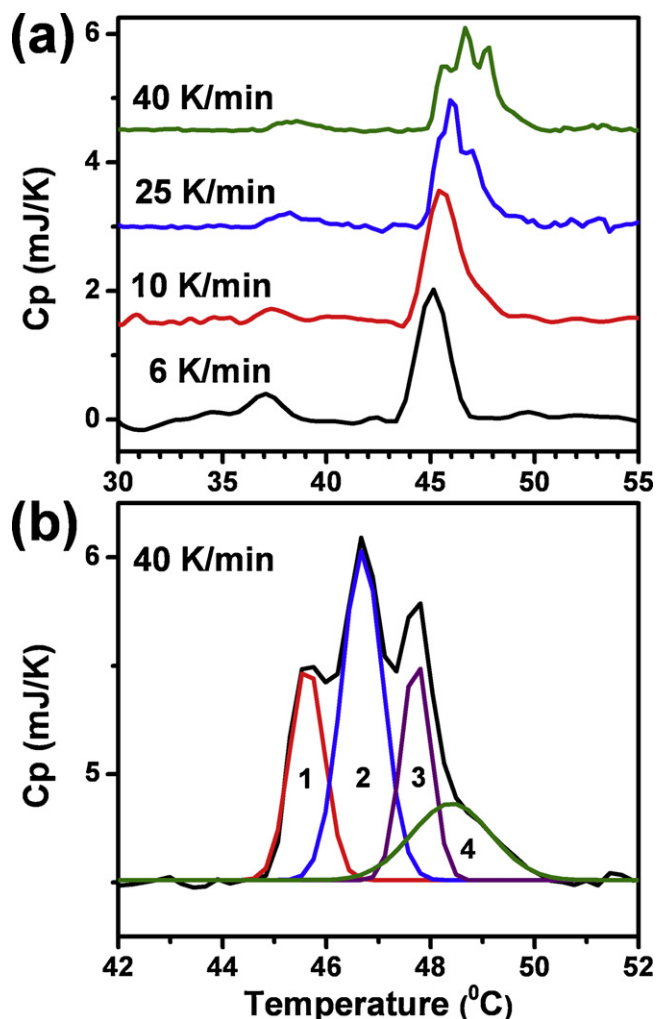


Fig. 4. (a) Heat capacity plot of 3 mM DODAB at different heating rates. Anomalous multiple peaks at the phase transition are observed at high heating rate. Only a single peak is present at slow heating rates using Microcal VP-DSC and our system. (b) The multiple peaks can be deconvoluted into four peaks using the multiple-peak fitting program in Origin™.

single (low scan rate) and multiple (high scan rate) transitions. We do not attribute this effect to instrumentation artifacts (e.g. temperature, resolution, thermal uniformity) as evidenced by the subgel transition (37 °C) which remains relatively invariant to scan rate.

We suggest that the overall transition of DODAB is actually comprised of multiple (at least 4) transitions that occur at all scan rates. At low scan rates, only a single peak is observed due to the inherent broadness of the transitions themselves. Even when using the Microcal™ VP-DSC system with a temperature resolution of 0.5 °C, only a single peak (FWHM ~ 1.4 °C) is observed. However at high scan rates the kinetic attributes of each individual process are sufficiently different so as to allow just enough time/temperature separation for the transitions to be resolved. Experiments of the protein samples have not yet been done at these high rates.

To our knowledge, this effect of peak separation has not been reported to date. We offer two possible models for the effect. The first is based on the presence of multiple domains/regions in the typical single-bilayer vesicle, whereas the second model suggests that the sample consists of vesicles with four different wall thicknesses (1-bilayer to 4-bilayers).

The first idea is that the melting transition may not occur in a single step due to distinct domains present in the bilayer structure. Recent studies on the liquid crystal to coagel phase transformation of DODAB show a non-synchronous behavior between the tail and head groups due to different interactions with the environment. This behavior suggests the presence of distinct segments within the DODAB bilayer which could melt at different temperatures [24]. Molecular dynamic simulations also show that the bilayer exists in a “ripple” like arrangement where two distinct domains are present; the “zipped” domain where the long alkane chains of the upper and lower monolayers are interdigitated with a thickness of 2.4 nm and an “unzipped” domain where the monolayers are separated by a distance with a thickness of 4.0 nm. The individual DODAB molecule also has different domains. The carbon atoms closest to the N head group (C1–C5) are less ordered compared to the extended chain (C6–C17) [25].

The second idea is based on the nature of size-dependent properties of materials. It is proposed that the material is composed of vesicles with walls composed of different number of bilayers. Typical DODAB solutions contain vesicles with walls of 1-bilayer, 2-bilayers, or larger multilayers of DODAB as well as bilayer fragments [20,26]. The distribution of thicknesses in the initial sample solution depends on the synthesis method. We suggest that our solution contains a distribution of four different layer thicknesses (1-layer to 4-layer) and are observed as the 4 different maxima in the C_p data obtained at high heating rates. This size-dependent melting phenomenon is well known for layered lamellar structures: thin layers melt at lower temperatures compared to thick layers [27,28].

Single-bilayer vesicles are the most common type of vesicles and are expected to be the most stable. The size of the vesicles may not be static, e.g. sonication can dramatically change the size distribution [26]. In our case individual vesicles may change in time due to the phenomenon of “swelling”; liquid passing into the interior region through the DODAB membrane. Swelling inherently increases membrane surface area and at the same time decreases layer thickness. We note that the reverse process (shrinking of vesicles) has also been observed, e.g. water depleted (evaporation) from the vesicle produces dry multilayer vesicles (empty) shells which give rise to lamellar reflections in XRD studies [29].

The calorimetry scanning rate is important because it controls the dynamics/kinetics of swelling. At low scan rates swelling of the vesicle allows all of the metastable multilayered vesicles to transform into the most stable single-bilayer vesicles. Therefore at low scan rates we observe only one melting point since all of the vesicles will be 1-bilayer vesicles. However at high heating rates calorime-

try captures the system before appreciable swelling occurs and thus four different melting temperatures are observed. As expected no additional melting peaks are observed when scanning at even faster rates since only four different sizes are present in the original solution.

There are other examples of systems which also show multiple discrete size distributions in both gas clusters [30] as well as surface clusters [31,32] of metals. Magic sizes are observed in metal [15] as well as layered silver thiolate systems [18,33] using nanocalorimetry [15], which is an analogous system to the one used in this study.

4. Conclusion

In summary, we have developed a capillary based calorimeter with 30 μ L sample volume. The device also achieved the fastest heating rate of 60 K/min reported for a liquid calorimeter. At high heating rates an anomalous presence of multiple peaks are observed for the DODAB phase transition. At low scan rates the phase transition temperature and heat of fusion of DODAB, Rnase A, Lysozyme and Cytochrome P450 are consistent with reported values using Microcal VP-DSC.

Acknowledgements

This study is supported by NSF ECCS 0622117. The materials analysis work is supported by NSF DMR 1006385. Microcal VP-DSC measurement is done at the University of Chicago Biophysics Core Facility. Some DSC measurement for DODAB provided by MicrocalTM (Cambridge, MA).

References

- [1] N.D. Socci, J.N. Onuchic, P.G. Wolynes, *Proteins* 32 (1998) 136.
- [2] R. Zhou, M. Eleftheriou, C. Hon, R. Germain, A. Royyuru, B. Berne, *IBM J. Res. Dev.* 52 (2008) 19.
- [3] W. Pfeil, B.O. Noelling, C. Jung, *Biochemistry* 32 (1993) 8856.
- [4] Y.Y. Zhang, S. Tadigadapa, *Appl. Phys. Lett.* 86 (2005) 030401.
- [5] L. Wang, B. Wang, Q. Lin, *Sens. Actuators B: Chem.* 134 (2008) 953.
- [6] J. Xu, R. Reiserer, J. Tellinghuisen, J. Wikswo, F. Baudenbacher, *Anal. Chem.* 80 (2008) 2728.
- [7] F.E. Torres, P. Kuhn, D.D. Bruyker, A.G. Bell, M.V. Wolkin, E. Peeters, J.R. Williamson, G.B. Anderson, J.P. Schmitz, M.I. Recht, S. Schweizer, L.G. Scott, J.H. Ho, S.A. Elrod, P.G. Schultz, R.A. Lerner, R.H. Bruce, *Proc. Natl. Acad. Sci.* 101 (2004) 9517.
- [8] W. Lee, W. Fon, B. Axelrod, M. Roukes, *Proc. Natl. Acad. Sci.* 106 (2009) 15225.
- [9] J.-L. Garden, E. Chateau, J. Chaussy, *Appl. Phys. Lett.* 84 (2004) 3597.
- [10] E.A. Olson, M.Y. Efremov, A.T. Kwan, S. Lai, V. Petrova, F. Schiettekatte, J.T. Warren, M. Zhang, L.H. Allen, *Appl. Phys. Lett.* 77 (2000) 2671.
- [11] M.Y. Efremov, E.A. Olson, M. Zhang, S. Lai, F. Schiettekatte, Z.S. Zhang, L.H. Allen, *Thermochim. Acta* 412 (2004) 13.
- [12] M.Y. Efremov, E.A. Olson, M. Zhang, F. Schiettekatte, Z.S. Zhang, L.H. Allen, *Rev. Sci. Instrum.* 75 (2004) 179.
- [13] S.L. Lai, G. Ramanath, L.H. Allen, P. Infante, Z. Ma, *Appl. Phys. Lett.* 67 (1995) 1229.
- [14] S.L. Lai, J.R.A. Carlsson, L.H. Allen, *Appl. Phys. Lett.* 72 (1998) 1098.
- [15] M.Y. Efremov, F. Schiettekatte, M. Zhang, E.A. Olson, A.T. Kwan, R.S. Berry, L.H. Allen, *Phys. Rev. Lett.* 85 (2000) 3560.
- [16] M.Y. Efremov, E.A. Olson, M. Zhang, Z. Zhang, L.H. Allen, *Phys. Rev. Lett.* 91 (2003) 85703.
- [17] L. Hu, Z.S. Zhang, M. Zhang, M.Y. Efremov, E.A. Olson, L.P. de la Rama, R.K. Kummamuru, L.H. Allen, *Langmuir* 25 (2009) 9585.
- [18] L. Hu, L.P. de la Rama, M.Y. Efremov, Y. Anahory, F. Schiettekatte, L.H. Allen, *J. Am. Chem. Soc.* 133 (2011) 4367.
- [19] F.R. Alves, E. Feitosa, *Thermochim. Acta* 472 (2008) 41.
- [20] E. Feitosa, P.C.A. Barreleiro, G. Olofsson, *Chem. Phys. Lipids* 105 (2000) 201.
- [21] I.G. Denisov, T.M. Makris, S.G. Sligar, I. Schlichting, *Chem. Rev.* 105 (2005) 2253.
- [22] M. Blandamer, B. Briggs, P. Cullis, J. Engberts, *Chem. Soc. Rev.* 24 (1995) 251.
- [23] P. Saveyn, P. Van der Meeren, M. Zackrisson, T. Narayanan, U. Olsson, *Soft Matter* 5 (2009) 1735.
- [24] F. Wu, N. Wang, Z. Yu, *Langmuir* 25 (2009) 13394.
- [25] D. Jamroz, M. Kepczynski, M. Nowakowska, *Langmuir* 26 (2010) 15076.
- [26] E. Feitosa, W. Brown, *Langmuir* 13 (1997) 4810.
- [27] B. Wunderlich, G. Czornyj, *Macromolecules* 10 (1977) 906.
- [28] J. Hoffman, J. Weeks, *J. Chem. Phys.* 42 (1965) 4301.
- [29] R. Ionov, A. Angelova, *Thin Solid Films: Seventh International Conference on Organized Molecular Films*, vol. 284–285, 1996, p. 809.
- [30] W.D. Knight, K. Clemenger, W.A. Deheer, W.A. Saunders, M.Y. Chou, M.L. Cohen, *Phys. Rev. Lett.* 52 (1984) 2141.
- [31] C.L. Cleveland, U. Landman, T.G. Schaaff, M.N. Shafiqullin, P.W. Stephens, R.L. Whetten, *Phys. Rev. Lett.* 79 (1997) 1873.
- [32] P.D. Jadzinsky, G. Calero, C.J. Ackerson, D.A. Bushnell, R.D. Kornberg, *Science* 318 (2007) 430.
- [33] L. Hu, L. De La Rama, M.Y. Efremov, L.H. Allen, in preparation.